



**Original Research Article**

## **In-Situ Polymerization of UHMWPE Using Bi-Supported Ziegler-Natta Catalyst of MoS<sub>2</sub> Oxide/MgCl<sub>2</sub> (Ethoxide Type)/TiCl<sub>4</sub>/TiBA: Study of Thermo-Mechanical Properties of System**

**Majed Amini<sup>1</sup>, Ahmad Ramazani S. A<sup>2</sup>\*, Amanj Kheradmand<sup>3</sup>**

<sup>1</sup>Chemical and Petroleum Engineering Department, Sharif University of Technology, Tehran, Iran

<sup>2</sup>Chemical and Petroleum Engineering Department, Sharif University of Technology, Tehran, Iran,

<sup>3</sup>Chemical and Petroleum Engineering Department, Sharif University of Technology, Tehran, Iran,

\*Corresponding author \*E-mail: [ramazani@sharif.edu](mailto:ramazani@sharif.edu)

---

### **ABSTRACT**

The use of UHMWPE has attracted the attention of many researchers and industries. The aim of the present work is to fabricate UHMWPE/MoS<sub>2</sub>-Oxide nano-composites using in-situ polymerization. For this purpose, modified molybdenum disulfide was used. In order to perform the polymerization, a Ziegler-Natta catalytic system, with MoS<sub>2</sub>-Oxide and magnesium Ethoxide as support, was used. In order to fabricate nano-composites with different filler percentages, the length of polymerization was varied while other parameters were constant. A significant increase in some of the mechanical properties such as modulus and yield stress confirms the effectiveness of interactions between the nano-particles and the matrix. Thermal properties of the obtained nano-particles were analyzed by DSC and TGA analysis. Results of these analyses indicate an increase in crystallinity, melting temperature and improvement in thermal stability of the

samples. Mechanical properties analysis indicates a significant increase in the modulus and tensile strength of nano-composites containing filler compared with pure polymer.

**Keywords:** in-situ polymerization, UHMWPE, nano-composite, MoS<sub>2</sub>-Oxide, Ziegler-Natta catalysis.

---

## Introduction

Nowadays, layered nano-particles are interesting because of their specific structure and significant properties. This type of fillers, which are in the form of sheets, exhibit much higher strength than fillers in particle or fiber form [1]. This is because these fillers are located in the direction of two main axes. The most important layered nano-particles are graphene, molybdenum disulfide and clay [2]. MoS<sub>2</sub> is a hexagonal material in which layers with weak molecular force are adjacent to each other and can easily slip on each other; therefore, MoS<sub>2</sub> has very good lubricating properties [3]. Neat MoS<sub>2</sub> cannot interact properly with a matrix, because it inherently tends to accumulate in the polymeric matrix that is why it needs to be modified [4–6]. Oxidation along with chemical functionalization can lead to the separation of MoS<sub>2</sub> layers [7–9], which helps the monomer to penetrate among the layers in an in-situ polymerization reaction [10,11]. By creating functional bonds, it is also possible to create strong bonding with polymer chains [12–14]. A lot of research has been conducted on Ziegler-Natta catalysts and in-situ polymerization reactions using these catalysts in recent decades. Rang et al. [15] fabricated polyethylene/ Palygorskite in 2001 using in-situ polymerization. First they placed the Ziegler-Natta catalyst on nano-fibers and began to polymerize the ethylene from the filler surface. They found that the co-catalyst plays a very important role in the polymerization process. An optimum Al/Ti molar ratio of 10 was obtained to get the highest polymer yield using an Al(i-Bu)<sub>3</sub> catalyst. Zohuri et al. [16] produced polyethylene using ethylene slurry polymerization with a Ziegler-Natta catalyst and two supports (SiO<sub>2</sub> / MgCl<sub>2</sub> / TiCl<sub>4</sub> / TEA). They used SiO<sub>2</sub> and Mg (OEt)<sub>2</sub> as supports for the catalyst and tri-ethyl aluminum as the co-catalyst. Lee et al. [17] produced polyethylene/montmorillonite nanocomposites using in-situ polymerization and a catalyst support system. They used methyl aluminoxane (MAO) as co-catalyst and Cp<sub>2</sub>ZrCl<sub>2</sub> as catalyst.

XRD results showed that the MMT layers were well laminated. Dashti et al. [18] investigated the kinetics and morphology of polypropylene nanocomposites produced by the Ziegler-Natta process. In their work, they investigated two different catalytic systems, one in the presence of an internal donor and one without the presence of the internal donor. The results for the effect of time on catalytic activity showed that, over time the activity increased and then decreased, which showed the catalyst was deactivated over time. Bahrami et al. [19–22] investigated the mechanical properties of polyethylene/graphene nanocomposites. The results of the tensile tests and the mechanical properties of the samples showed that with increasing nanoparticle content, the tensile strength and Young's modulus increased for all samples. The number of articles and researches in recent years on the production of UHMWPE shows the importance of this topic in research and industry. But an overview of studies indicates that there are still good research opening in this area. The fabrication of UHMWPE / MoS<sub>2</sub>-Oxide nanocomposites has not been well investigated. Hence, in this study, modified MoS<sub>2</sub> nano-particles were used as a reinforcing component as well as a catalyst support in the polymerization process of UHMWPE. Hence, modified MoS<sub>2</sub>, obtained in the previous work of this research group [3], was used to synthesize ultra-high-molecular-weight polyethylene nanocomposites, and the effect of this nanoparticle on the physical, mechanical and thermal properties of the nanocomposites was investigated.

## EXPERIMENTAL SECTION

### Materials

Table 1 displays the materials used in this study, along with the chemical formula, the manufacturer, and the role of these materials in the production of samples and their purity. Modified molybdenum disulfide, used in this study, is selected based on a previous study of this research group [3].

**Table 1.** The consumed materials with supplier, application and their purity.

Material	Chemical Formula	Supplier	Application	Purity (%)
<b>Molybdenum Disulfide Oxide</b>	MoS <sub>2</sub> O	Previous work [3]	-	>97
<b>Argon</b>	Ar	Arkan Gas Co.	Inert Gas	99.9999
<b>Ethylene</b>	C <sub>2</sub> H <sub>4</sub>	Jam Petrochemical Co.	Monomer	99
<b>Titanium Tetrachloride</b>	TiCl <sub>4</sub>	Merck	Catalyst	99
<b>Triisobutylaluminum</b>	TIBA	Sigma Aldrich	Co-Catalyst	96
<b>Dibutyl Phthalate</b>	DIBP	Merck	Internal Donor	99
<b>Molecular sieve and Silica Gel</b>	-	Pars Shimi Co.	Moisture Absorption	-
<b>Magnesium Ethoxide</b>	Mg(OEt) <sub>2</sub>	Sigma Aldrich	Catalyst Support	95
<b>Hexane</b>	C <sub>6</sub> H <sub>14</sub>	Kermanshah Petrochemical Industries Co.	Solvent	99.99
<b>Toluene</b>	C <sub>7</sub> H <sub>8</sub>	Merck	Solvent	99

### Preparation of Zeigler-Natta catalyst

The components of a nano-catalyst performance system for UHMWPE production comprise several parts including a feed gas capsule, gas flowmeters, a high pressure reactor, a heater to supply the reaction heat and a pressure control device. Catalyst tests were conducted in a reactor containing a few grams of the synthesized catalyst in neutral gas condition and at a temperature range of 60-70 °C. A continuous stream of ethylene was injected into the reactor. Purified hexane was used as a solvent in the reaction medium. In order to absorb the water in hexane and purify it, hexane is heated in the reflux distillation system adjacent to sodium. Molecular sieve and silica gel columns were used to purify the gas flow before use and they were placed in the path of the gas. The reactor used for polymerization is Buchi Glass. In the Ziegler-Natta processes, it is crucial that the water and moisture level must be low, because the polymerization is only possible in very low humidity, which is why the dewatering stage is very important. Therefore, before starting the catalyst support process, MoS<sub>2</sub>-Oxide was calcined at a temperature of 120 °C for 6 hours in a furnace. Solvent purification is also crucial; therefore the solvent, in the presence of sodium, was heated in a reflux distillation system to absorb the water contained therein under the inert gas of argon. In order to prevent the oxygen or water vapor entering the support system, a continuous stream of argon gas was entering the system. All operations have been performed in a Glove box and under an argon gas stream. 4 to 6 grams of MoS<sub>2</sub>-Oxide, after calcination at 150 °C for 6 hours, is poured into a two-span balloon made for

this purpose. The balloon is placed under argon to prevent air from entering. Then the balloon enters the Glove Box and 1 to 2 grams Mg (OEt)<sub>2</sub> is added. To the resulting mixture, 80 cc of toluene is added as a solvent to the reaction medium. Then, to the resulting suspension 8 mL of TiCl<sub>4</sub> and 2 mL of internal donor (di-isobutyl phthalate) are added. The balloon is placed in the oil bath and after reaching the temperature a 115 °C, the mixture is stirred for 12 hours. The aim of stirring is to increase the contact surface for better reaction. It should be noted that the entire system is under the inert gas of argon to prevent air from entering the system. After the desired time, in order to remove the unreacted Titanium from the system, the obtained suspension is washed three times with fresh hexane. The residual product is used as a catalyst for polymerization of ethylene.

### In-situ polymerization

In order to clean the reactor from possible contamination and to remove moisture and air from the reactor, the reactor preparation should be done at the beginning of the work. At this stage, the reactor is first filled with argon gas and evacuated after 5 minutes. This should be done twice. Due to the gas form of the monomers and the presence of a solid phase in the catalyst, in order to establish contact between the two phases and perform the polymerization, hexane was added to the system. At this stage, 300 mL of solvent is injected into the reactor. Then 2 to 4 mL of the cocatalyst is injected into the reactor. This step takes about 10 minutes and the reactor temperature should be adjusted to 60 °C. At the end of this time period, the catalyst is injected into the reactor and the polymerization begins with the addition of monomer into the reactor. Gas monomers are first dissolved in hexane and then introduced into the polymerization reaction. For this purpose, the stirring rate is 700 rpm. Gas consumption and an increase in system temperature indicate the initiation of a polymerization reaction in the reactor. In the polymerization reaction, the  $\pi$  carbon bonds are converted to  $\delta$  [10], which is the reason for heat production and an increase in the temperature of the system. After the end of the polymerization period, the catalyst still maintains its activity; therefore, to deactivate it, a portion of a dilute solution of chloride acid in ethanol is added to the system. The resulting nanocomposites are powdery. After separating them from the solvent using a filter paper, they are rinsed several times with ethanol and then hexane and finally filtered and, in order to remove the total alcohol and hexane from the powdered nanocomposite grains, for 24 hours they are placed in vacuum at 70 °C. Finally, depending on the amount of output, the percentage of nanoparticles in the polymer matrix is

determined. In this study, 5 samples were prepared containing zero percent of nanoparticles, 0.47%, 1.1%, 1.67% and 2.08%, with the codes A, B, C, D, E, respectively.

### **Techniques and analysis**

Various tests were used to determine the characteristics and specifications of the obtained nanocomposites, including:

#### **ICP-OES analysis**

An ICP-OES test was used to obtain the amount of Supported titanium in the catalysis. The model of the device is VISTA-PRO from the Australian Varian Company.

#### **FTIR analysis**

The FTIR analysis is a suitable method for identifying raw materials and identifying existing functional groups on the surface. The FTIR analysis for each sample was performed using the ABB Bomem MB-100 spectrometer.

#### **FE-SEM**

Samples for FE-SEM imaging should be free from moisture, organic solvents and oily layers. The FE-SEM analysis was carried out using a TESCAN-MIRA iii, manufactured in the Czech Republic. Since these samples are non-conductive, they were coated with gold.

#### **Average molecular weight measurements of UHMWPE nanocomposites**

In order to determine the molecular weight of the obtained samples, using the intrinsic viscosity and the Mark-Houwink equation, a certain amount of polymer powder is dissolved in Decalin solvent at 150 °C for 1 hour, then the solution poured inside the Ubbelohde viscometer, which is in the oil bath at 140 °C. The times required for the fall of a certain volume of the solution in the narrow tube of the viscometer are measured and the intrinsic viscosity can be obtained using the following equations: (1) & (2)

$$\eta_r = \frac{\frac{t_s - K}{t_s}}{\frac{t_0 - K}{t_0}} = \eta_{sp} + 1 \quad (1)$$

$$[\eta] = \frac{(2\eta_{sp} - 2 \ln \eta_r)^{0.5}}{C} \quad (2)$$

where K is the viscometer constant and  $\eta_r$  and  $\eta_{sp}$  are the relative and specific viscosity, respectively.  $t_0$  is the fall time of the pure solvent and the  $t_s$  is the fall time of the polymer solution. Finally, the calculated inherent viscosity is related to the Mark-Houwink relationship (Eq. 3) in order to obtain the molecular weight [11]:

$$M_v = 5.37 \times 10^4 [\eta]^{1.37} \quad (3)$$

where  $M_v$  is the molecular weight and  $[\eta]$  is the intrinsic viscosity. 1.37 and  $5.37 \times 10^4$  are the constants of the Mark-Houwink equation in this system.

### Tensile analysis

Hounsfield h10ks were used to perform the tensile test. The tensile test was carried out according to the ASTM D638 standard. The tensile strength of the sample was studied along with other mechanical properties such as the strain and modulus in stretching mode (Young's modulus).

### DSC analysis

DSC analysis was used to investigate the effect of the nanoparticles on the UHMWPE glass transition temperature. The device used was of the Q100 type manufactured by TA Instruments in the United States of America. The accuracy of this device is 0.1 °C and the transferred heat is measured with 0.1 watt per milligram accuracy. To obtain the glass transition temperature of pure and modified polyethylene with MoS<sub>2</sub>-Oxide nanoparticles, 10 mg of pure polymer as well as polymer containing various percentages of nanoparticles were placed in aluminum containers of the device at a rate of 10 degrees per minute from ambient temperature up to 200 °C and then cooled down to 20 °C in the second stage.

### TGA analysis

TGA analysis was conducted to investigate the effect of nanoparticles on the thermal degradation of pure polyethylene and polyethylene containing nanoparticles. The device is STA PT1600, manufactured by LINSEIS in the United States of America. To determine the amount of coal in nitrogen atmosphere, the samples were first placed in a vacuum oven for 1 hour at 50 °C to evaporate the volatile components such as residual water and unreacted monomer. Then 8 mg of

each sample were placed inside the device and heated at the rate of 10 degrees per minute up to 700 °C.

## Results and Discussion

### Characterization of MoS<sub>2</sub> Oxide nameplates

As mentioned before, in the previous study of this group [3], the surface modification MoS<sub>2</sub>-Oxide was carried out with various methods. In the following, the general properties of the modified sample are mentioned. It should be noted that these properties of MoS<sub>2</sub> are used in the analysis of the obtained nanocomposites properties.

### FTIR results

The FTIR spectrum for modified molybdenum sulfide (MoS<sub>2</sub>-Bulk) and modified (MoS<sub>2</sub>-Oxide) in the range of 4000-400 cm<sup>-1</sup> wavelengths is shown in Figure 1.

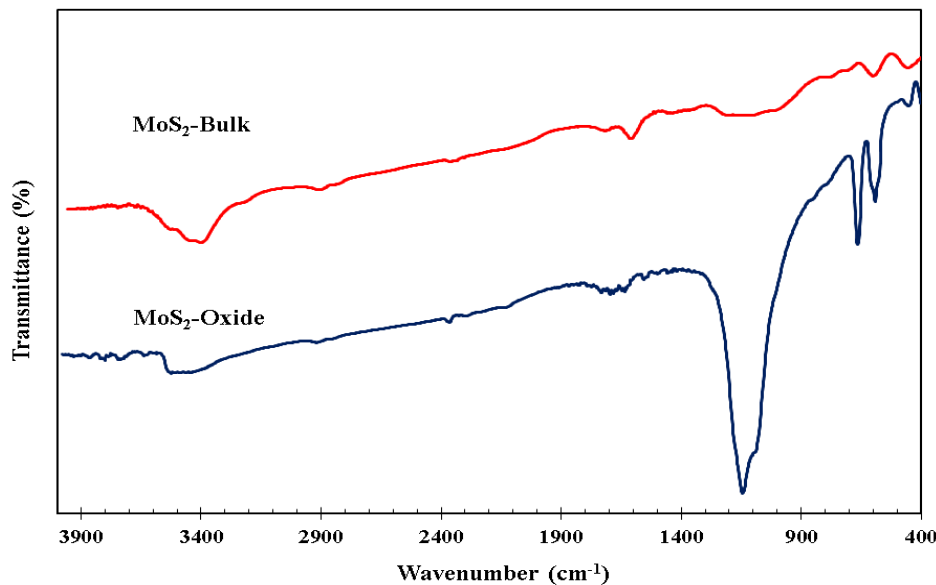


**Figure 1.** FTIR spectrum of MoS<sub>2</sub> and MoS<sub>2</sub>-Oxide.

From Figure 1, it can be seen that the molybdenum sulfide unmodified sample has no functional groups and only one small peak in the wave number at about 134 cm<sup>-1</sup>, which is related to the OH group, and represents the small moisture content in the sample. As stated above, in in-situ polymerization, the presence of a functional group in nanoparticles has a strong positive effect

on the final properties. For this reason, the modification of  $\text{MoS}_2$  and the formation of functional groups, especially  $\text{S}=\text{O}$ , can be effective in catalytic polymerization reactions [3,11,12,14,23]. By performing the appropriate oxidation and washing, the mentioned bond was definitely established, and the presence of a peak at a wave number of about  $1110 \text{ cm}^{-1}$  in an oxidized sample verifies this claim [24,25].

### XRD results

Figure 2 shows the X-ray diffraction patterns of unmodified and modified  $\text{MoS}_2$ . Available peaks at  $2\theta = 57.9^\circ$  and  $53.9^\circ$ ,  $49.2^\circ$ ,  $43.2^\circ$ ,  $38.9^\circ$ ,  $35.3^\circ$ ,  $33.0^\circ$ ,  $32.2^\circ$ ,  $28.6^\circ$  in the  $\text{MoS}_2$  sample indicate the presence of the layered structure at the beginning and before any intercalation process, which is related to the hexagonal structure of the specimen [3], (JCPDS:  $\text{MoS}_2$  No : 87-2416). In this figure, it can be noted that, in the modified sample, the peak at  $2\theta = 14^\circ$  is constant, and the only change is the decrease in peak intensity. This suggests that the overall structure of the  $\text{MoS}_2$  has maintained its regularity and stacks of layers are intact, but the development of a peak at  $2\theta$  below 10 degrees indicates the creation of a gap between the layers [3,26,10]. Increasing the peak intensity below  $10^\circ$ , which is known as the 001 peak, and shifting it to smaller angles clearly indicates an increase in the distance between the layers [13].

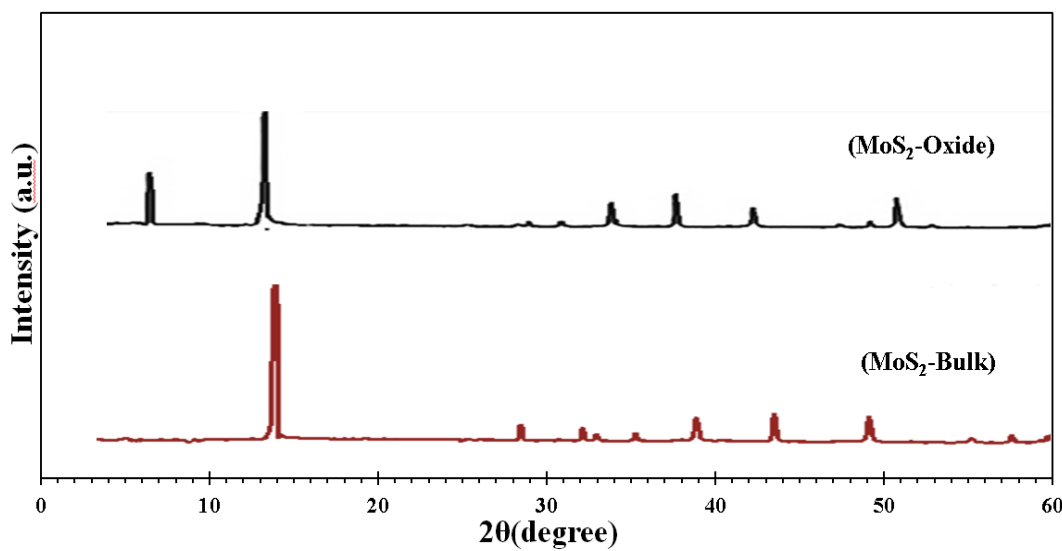


**Figure 2.** XRD spectrum of  $\text{MoS}_2$  and  $\text{MoS}_2$ -Oxide.

### Characterization of UHMWPE/MoS<sub>2</sub> nanocomposites

In the following section, the properties of UHMWPE/MoS<sub>2</sub> nano-composites are presented:

#### Average molecular weight measurement results

In Table 2, the average molecular weights (M<sub>v</sub>) of polymers are shown. As is known, sample A has the highest and sample E has the lowest molecular weight. The reason is the presence of MoS<sub>2</sub> nanoparticles in the catalyst support. The addition of nanoparticles to the polymer matrix during the polymerization process prevents the growth of chains and, therefore, from a certain limit, the growth of chains is stopped and the molecular weight is lower than the pure polymer. This is very important in the reformation of UHMWPE, since it is very difficult to reform these materials. In our study, not only did we reduce the average molecular weight of the nanocomposites, which makes them easier to process [27], but also we improved the mechanical and thermal properties. The results of the mechanical properties analysis are in the following sections.

**Table 2.** The average molecular weight (M<sub>v</sub>) of samples.

Sample	(A)	(B)	(C)	(D)	(E)
M <sub>v</sub> (Million gram/mol)	4.37	4.02	3.74	3.15	2.85

#### ICP-OES analysis

In order to determine the quantity of supported titanium in the obtained catalyst, the ICP method was used to elemental analysis of most of the element. Here, the catalyst activity is reported as

$\frac{\text{gr. PE}}{\text{mmol Ti.h}}$ . The molar quantity of titanium in the catalyst is calculated through the ICP test and the

aluminum quantity is calculated by the amount of cocatalyst input in the reactor. The molar ratio

of  $\frac{\text{Al}}{\text{Ti}}$  is an important factor in the efficiency of the catalyst whose role is to remove the impurities and reduce  $\text{Ti}^{4+}$ . To investigate the effect of the  $\frac{\text{Al}}{\text{Ti}}$  molar ratio, polymerization was carried out at 60 °C for 60 minutes and 10 bar pressure in various  $\frac{\text{Al}}{\text{Ti}}$  molar ratios. Tables 3 and 4 show the experimental conditions to investigate the catalyst activity of  $\frac{\text{TiCl}_4}{\text{Mg(ETO)}_2}$  and  $\frac{\text{TiCl}_4}{\text{MoS}_2 - \text{Mg(ETO)}_2}$ .

**Table 3.** The experimental conditions to investigate the catalyst activity of  $\frac{\text{TiCl}_4}{\text{Mg(ETO)}_2}$  for UHMWPE production.

#	Ti (mmol)	Al (mmol)	Al/Ti	PE (gr)	$\bar{R}_p$ ( $\frac{\text{gr PE}}{\text{mmol Ti.hr}}$ )
1	0.108	13	120.37	220.87	2045.15
2	0.108	26	240.74	231.20	2140.79
3	0.108	39	361.11	217.21	2011.24
4	0.108	52	481.48	215.70	1997.31
5	0.108	65	601.85	212.22	1965.09

**Table 4.** The experimental conditions to investigate the catalyst activity of  $\frac{\text{TiCl}_4}{\text{MoS}_2 - \text{Mg(ETO)}_2}$  for UHMWPE production.

#	Ti (mmol)	Al (mmol)	Al/Ti	PE (gr)	$\bar{R}_p$ ( $\frac{\text{gr PE}}{\text{mmol Ti.hr}}$ )
1	0.0927	13	140.23	155.20	1674.25
2	0.0927	26	280.47	165.88	1789.48
3	0.0927	39	420.71	157.40	1697.97
4	0.0927	52	560.94	130.82	1411.28
5	0.0927	65	701.18	116.24	1254.01

Figure 3 shows the activity of the catalysts. As can be seen, with an increasing  $\frac{\text{Al}}{\text{Ti}}$  molar ratio, the catalyst efficiency first increases and then, after a specific value, it starts to decrease. The optimal molar ratios of  $\frac{\text{Al}}{\text{Ti}}$  for the  $\frac{\text{TiCl}_4}{\text{Mg(ETO)}_2}$  and  $\frac{\text{TiCl}_4}{\text{MoS}_2 - \text{Mg(ETO)}_2}$  catalysts are 240.74 and 280.47, respectively. At low concentrations of TIBA, system impurities affect the polymer

production, and active centers haven't activated yet. At higher concentrations than optimal quantities,  $Ti^{4+}$  may be reduced to  $Ti^{2+}$ , resulting in decreased activity of ethylene polymerization [14]. From Figure 3, it can be said that the catalyst is more active. This can be attributed to catalyst support. In a support system of magnesium Ethoxide, the amount of catalyst atoms ( $TiCl_4$ ) participating in the reaction is higher than with  $MoS_2$  support, which can lead to increase in polymer production. Table 5 shows the ICP test results. The synthesized catalysts are dried after several washings in hexane and then subjected to ICP testing. In the following, according to the results obtained for the catalyst activity, the best  $\frac{Al}{Ti}$  ratio is selected and, based on that constant ratio, all nanocomposite samples are synthesized.

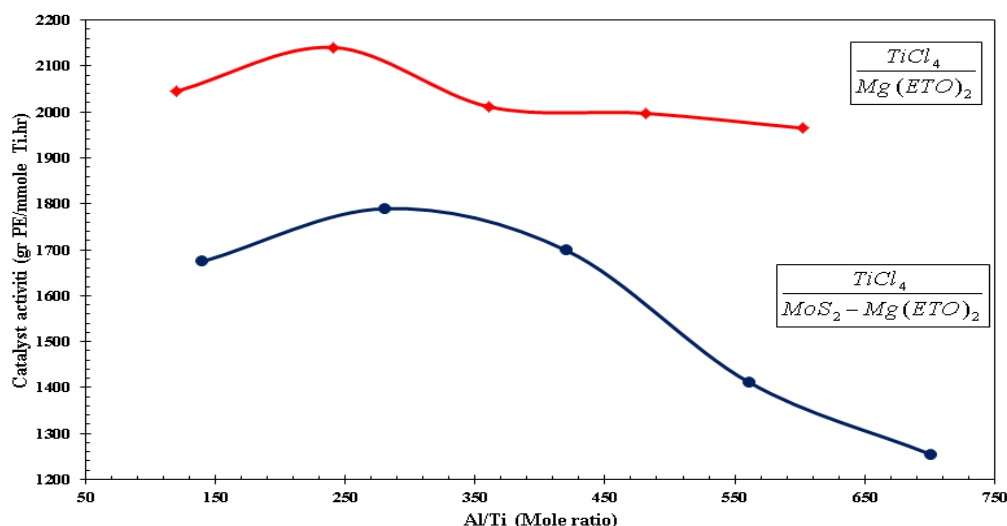


**Figure 3.** Effect of Al/Ti molar ratio on the catalyst activity of  $\frac{TiCl_4}{Mg(ETO)_2}$  and  $\frac{TiCl_4}{MoS_2 - Mg(ETO)_2}$ .

**Table 5.** Determine the amount of titanium in the synthesized catalysts

Catalyst	Titanium (wt.%)
$\frac{TiCl_4}{Mg(ETO)_2}$	4.7
$\frac{TiCl_4}{MoS_2 - Mg(ETO)_2}$	3.9

### FE-SEM Results

Proper distribution of filler in the polymer matrix is an important parameter to improve the mechanical properties and adhesion of the nanocomposites [28]. Because of this, FE-SEM images were used to determine the distribution of  $MoS_2$ -Oxide nanoparticles in the polyethylene

matrix. These images are taken from cross sections of pressurized molded nanocomposites, after fracturing inside the liquid nitrogen and coating with conductive gold. SEM images are shown in Figure 4 for two types of samples B and E. In order to analyze the images more accurately, the images from the fractured surface were taken with two different magnifications. All the SEM images indicate that the MoS<sub>2</sub> nano-layers have been dispersed properly in the matrix; and only the result for samples with low and high nano-layer content are shown because of the similarity in morphology of all samples.

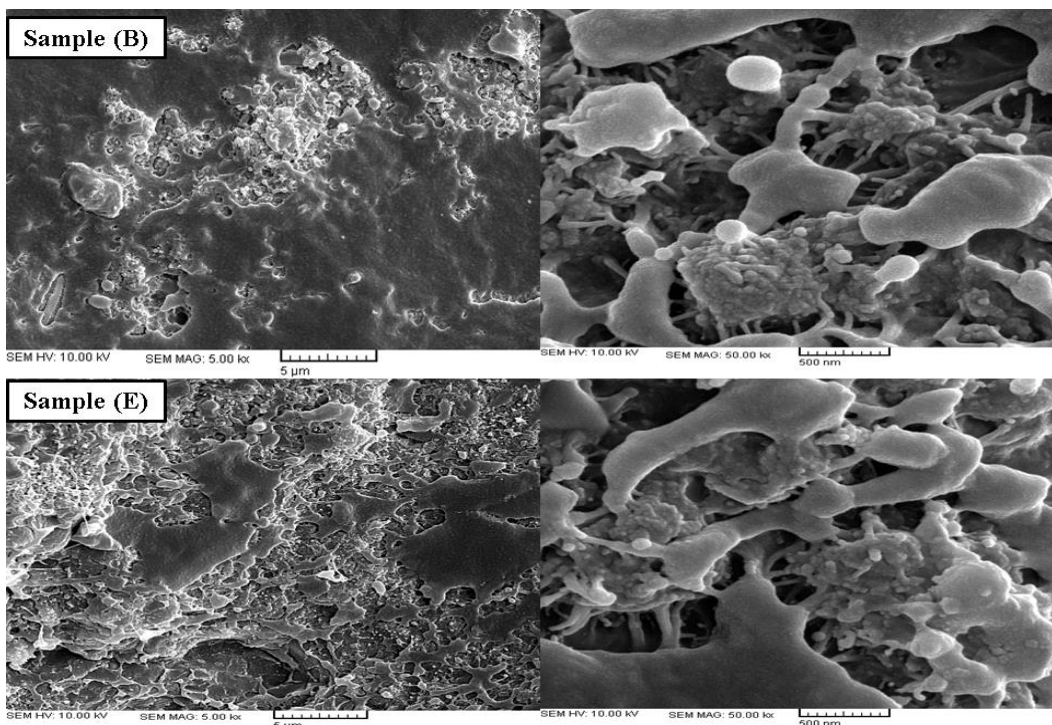


**Figure 4.** FE-SEM images of fractured surfaces of B (0.47 wt %) and E (2.08 wt %) samples.

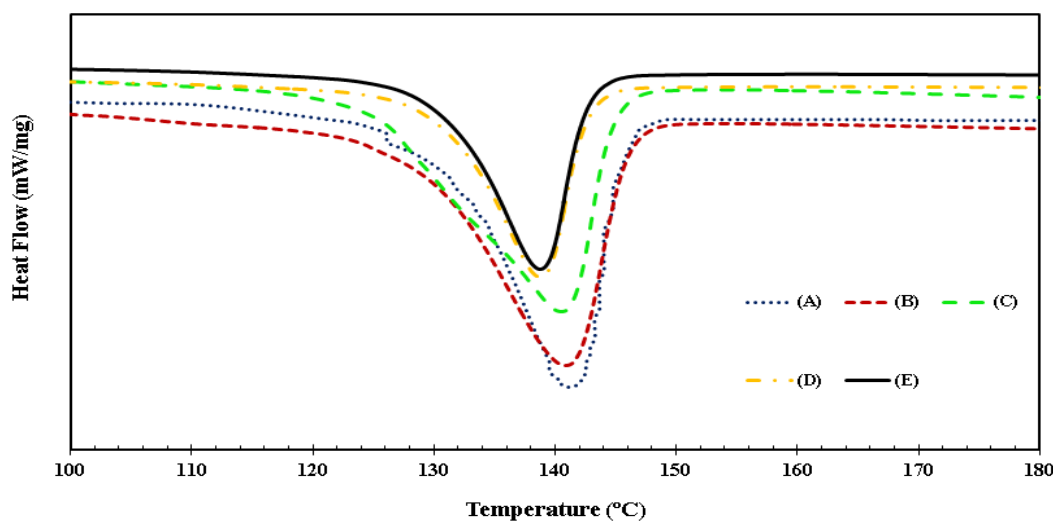
With the help of these images, the topography of the surface can also be analyzed. As can be seen in all the illustrations, the fractured surfaces are flat and smooth, indicating a high adhesion between the filler and the matrix. These images verify that the homogenous nanocomposite production in the in-situ polymerization method is due to better mixing and monomer growth in the interlayer space. The lack of a significant difference in all the SEM images for both low and high amount of MoS<sub>2</sub>-Oxide (0.47 and 2.08% by weight) indicates the uniform distribution of this filler in the polymer matrix. However, despite the choice of in-site polymerization as the method for fabricating the nanocomposites, with more uniform filler particle dispersion than

other methods, a few nanoparticle accumulations are inevitable due to the intense tendency of functional groups to accumulate.

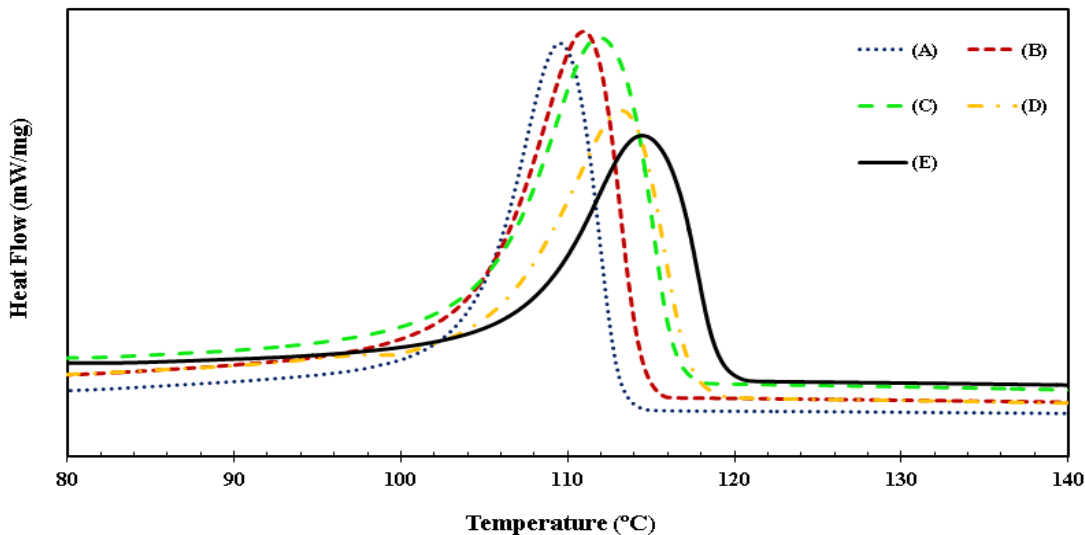
### DSC results

The presence of common surfaces (particles or other materials) may affect the mobility of molecular chains, especially those closer to the surface. If there is a strong bond between the polymer and the filler, this phenomenon reduces the glass transition temperature. From the structural viewpoint to the behavior and interaction of polyethylene chains and MoS<sub>2</sub>-Oxide nanoparticles, it can be deduced that the presence of nanoparticles along with polymer chains produces two main regions. A boundary region between the nanoparticles and polyethylene is created by the hydrogen bonds between polyethylene active functional groups and groups presented in nanoparticles surface. These bonds can significantly reduce the mobility of polymeric chains; by getting farther from the nanoparticle surface, the mobility of the chains increases and can be extended to a region that behaves like a pure polymer mass [29].

Figures 5 and 6 illustrate the DSC curves of pure polymer and fabricated nanocomposites. As can be seen, in the DSC curve of UHMWPE, there is an endothermic peak related to melting and a single exothermic peak related to crystallinity.



**Figure 5.** Endothermic DSC curves of A to E samples.

**Figure 6.** Exothermic DSC curves of A to E samples.

The results of DSC analysis for all samples are presented in Table 6. These results include the melting temperature ( $T_m$ ), crystalline temperature ( $T_c$ ), melting heat ( $\Delta H_f$ ) and crystallinity ( $X_c$ ).

**Table 6.** Results obtained from the DSC curve.

Sample	$T_m$ (°C)	$T_c$ (°C)	$\Delta H_f$ (J/g)	$X_c$ (%)
(A)	141.67	109.91	161.21	55.02
(B)	141.58	110.85	163.57	56.12
(C)	141.02	112.74	162.24	55.99
(D)	139.72	114.18	148.64	51.59
(E)	139.28	115.04	145.92	50.87

The crystallinity of the UHMWPE/MoS<sub>2</sub> nanocomposites can be calculated by the following expression [20]:

$$X_c = \frac{\Delta H_f}{(1 - \phi)\Delta H^\circ}$$

where  $\phi$  is the nanoparticle weight fraction and  $\Delta H^\circ$  is the melting heat of 100% crystalline polyethylene (equal to 293 J/g). The results of this test indicate an increase in crystallinity for the two lower percentages and a decrease for higher percentages. The increase in crystallinity for the lower percentages of MoS<sub>2</sub>-Oxide is because its surface acts as nucleation sites for crystallization, resulting in the nucleation and growth of crystals, which can lead to an increase in crystallinity. Although the MoS<sub>2</sub>-Oxide filler molecules act as nucleation sites, they reduce the

mobility of the polymeric chains and consequently inhibit the growth of crystallites. This is one of the reasons for lower crystallinity for higher percentages. The other reason for the reduction of crystallinity can be attributed to an increasing cooling rate during the formation process, which reduces the chains arrangement time to form crystallite.

### TGA results

The thermal stability of MoS<sub>2</sub> based nanocomposites in nitrogen atmospheric conditions with a temperature rate of 10 °C/min was evaluated using a thermal gravimetric analysis (Figure 7). As can be seen, all nanocomposites show a degradation peak at about 420-480 °C which is related to thermal degradation of polyethylene chains [30,31]. We can see that, with an increase in filler content, the polymer degradation temperature is shifted to higher temperatures. For instance, T<sub>0.05</sub> (temperature at which 5% degradation occurs) is 440.71, 41.44, 446, 184.44 and 459.24 °C for samples A to E, respectively. This improvement in thermal properties can be attributed to an increase in the thermal conductivity of nanocomposites in the presence of MoS<sub>2</sub>, which prevents heat accumulation in a region and prevents its degradation. The strong interaction between the matrix and the MoS<sub>2</sub>-Oxide nanoparticles in the interface, which confirmed by the FE-SEM images, reduces the mobility of polymeric chains, which would improve the thermal properties. It should be noted that in thermal degradation in the presence of oxygen, MoS<sub>2</sub> has a deterrent effect on oxygen penetration due to its plate-shape structure and delays polymer degradation. Improving the thermal stability of the synthesized nanocomposites is another reason for the proper dispersion of nanoparticles in the polymeric matrix.

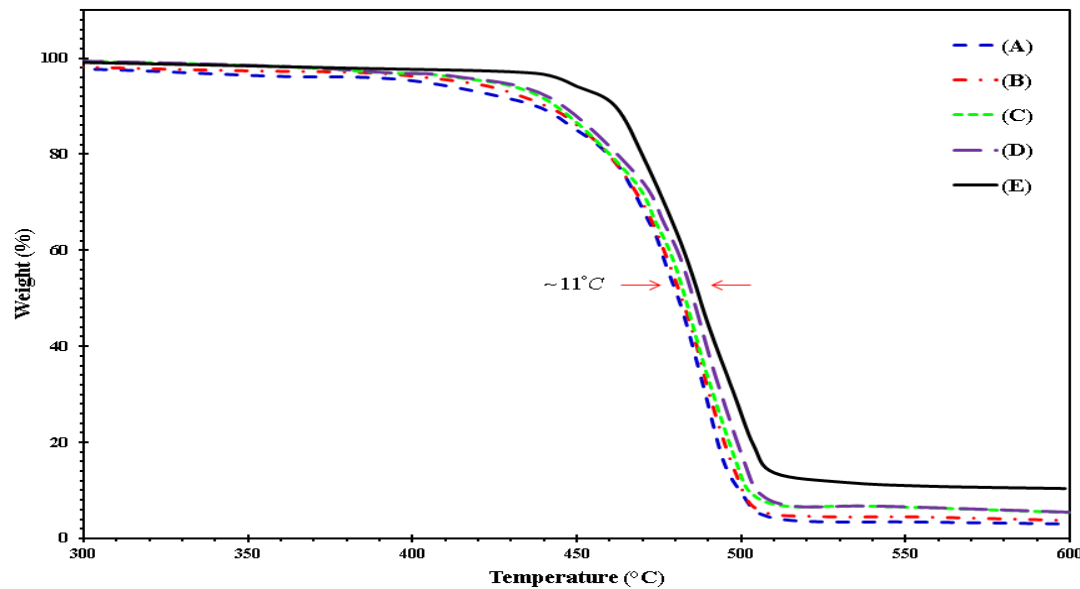
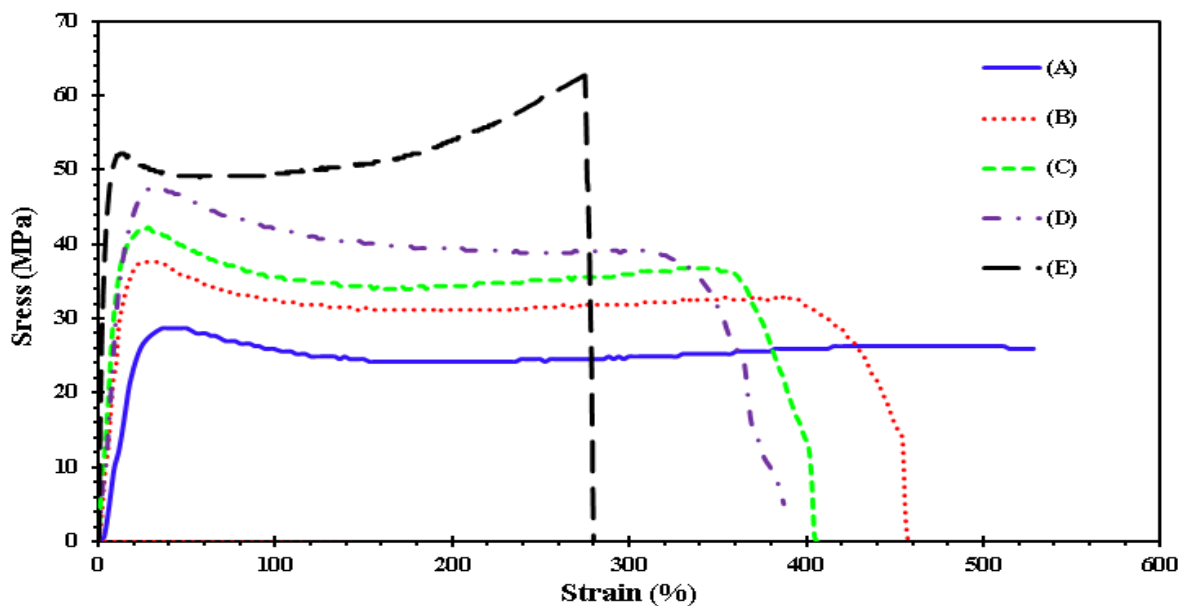


**Figure 7.** TGA thermographs of A to E samples.

### Tensile results

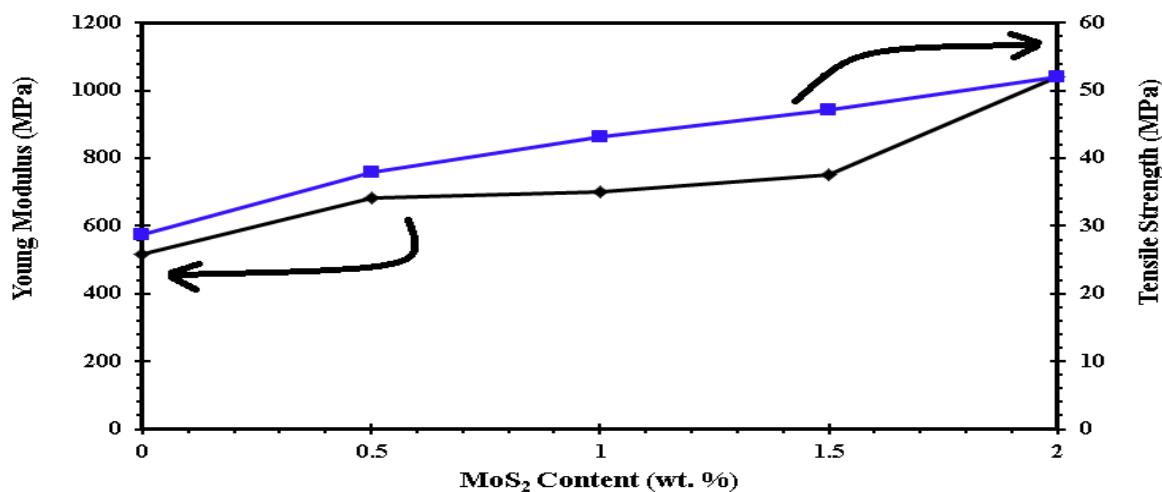
The semi-crystal polymer structure at the molecular scale consists of two phases: a crystalline phase and an amorphous phase. The crystalline region consists of lamella crystals with folded chains. The amorphous or interlayer region consists of four types of polymer molecules: 1) chain with a free head, 2) loop chains (the first and the end of the chain belongs to one lamella, 3) bonding molecules that are attached to two lamellas and 4) suspended molecules that are not attached to any of the lamellas [22,30]. Bonding molecules between the lamellas transfer the stress from one crystal to another crystal. UHMWPE has a long chain structure. In this type of polymer, the bonding chains play an important role in the polymer's tensile properties. The reason for the increase in modulus with decreasing molecular weight as the effect of nano-particle addition is that, with decreasing molecular weight, the length of the interconnecting chains decreases (decrease in the entanglement of bonding chains) causing these chains in the elastic region to play a greater role in increasing the modulus and strength. Due to the application of nanocomposites based on UHMWPE in various military industries and car frameworks, mechanical analysis has been carried out to evaluate the tensile properties of nanocomposites and also the effect of the nano-particle content on the performance of these materials.

The results of tensile analysis that were repeated three times for each sample can be seen in Figure 8, presenting the stress-strain curves obtained from pure polymer and nanocomposites.



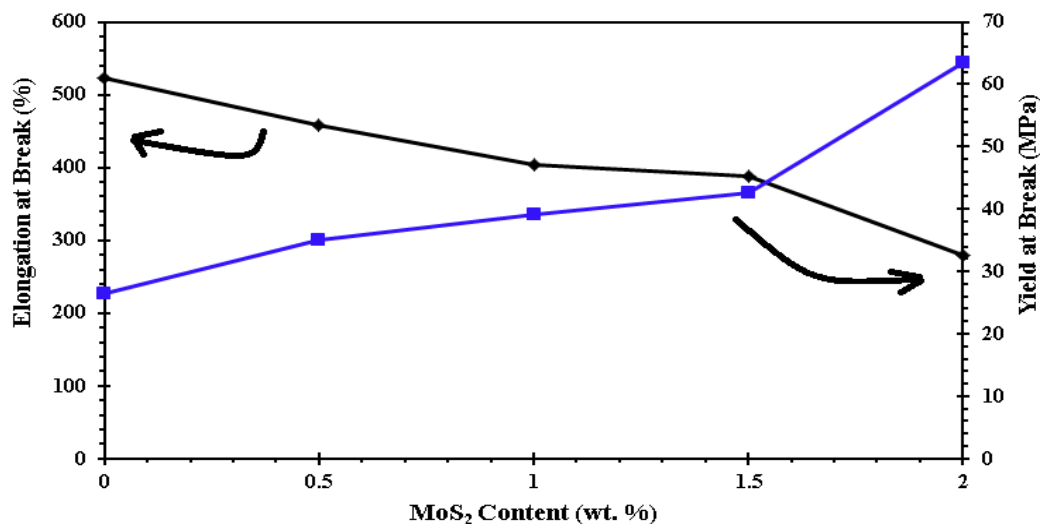
**Figure 8.** Stress-strain curves of A to E samples.

Figure 9 shows changes in the Young's modulus and tensile strength in terms of the MoS<sub>2</sub>-Oxide content. As can be seen, the Young's modulus (rigidity) increases with increasing filler content. Increase in the modulus by increasing the MoS<sub>2</sub>-Oxide content indicates a strong adhesion and homogeneous distribution of the filler in the polymer matrix. According to the results, the polymer strength is improved, especially with a lower content of MoS<sub>2</sub>-Oxide. Improvement in tensile strength by increasing the filler content also verifies the uniform distribution and strong adhesion between the filler and matrix. The other reason for the improvement in tensile strength, especially with low percentages, is attributed to an increase in crystallinity. Another reason for the improvement of the tensile properties of nanocomposites is the plate shape and the high aspect ratio of MoS<sub>2</sub>-Oxide.



**Figure 9.** Young's modulus and tensile strength of nanocomposites versus MoS<sub>2</sub> content.

Figure 10 shows the variation in the yield stress and the elongation of synthesized samples in terms of the weight percentage of MoS<sub>2</sub>-Oxide. As you can see, pure polymers have a lower yield stress due to their higher molecular weight. The reason for this is that, by increasing the molecular weight of the polymer and subsequently increasing the length of the chains and the bonding molecules, these molecules have less effect on the yield stress in the elastic region. Another point that can be deduced from the results is that the strain variation at the breaking point in terms of the weight percentage of MoS<sub>2</sub>-Oxide indicates that, by increasing the nanoparticle content even at low percentages, the elongation at the break has decreased. The reason for this is that, as a result of increasing the MoS<sub>2</sub>-Oxide content, the mobility of the polymeric chains decreases and therefore the elongation decreases in the plastic region.



**Figure 10.** Elongation and yield at break of nanocomposites versus MoS<sub>2</sub> content.

### Conclusion

In this study, modified MoS<sub>2</sub> nanoparticles are used to fabricate UHMWPE nanocomposites by in situ polymerization. The results of morphological observations showed that the MoS<sub>2</sub>-Oxide nano-sheets have been properly dispersed in the matrix. Crystallinity analysis of samples indicates an increase in crystallinity with a low content of MoS<sub>2</sub>-Oxide. The study of mechanical properties also confirms that the presence of MoS<sub>2</sub>, even at low percentages, improves tensile properties, such as the Young's modulus, yield stress and maximum stress. The reason for the improvement of these properties can be seen in the good adhesion of the filler and the matrix, the strength and high aspect ratio of MoS<sub>2</sub>, proper dispersion of MoS<sub>2</sub> and increased crystallinity. Also, the improvement of the thermal stability of nanocomposites produced in comparison with pure polymer was confirmed by thermo-gravimetric analysis. The results of this study show that the in situ polymerization method using Ziegler-Natta catalysts is a suitable method for the fabrication of UHMWPE, and MoS<sub>2</sub> nanocomposites can be used as an ideal filler for improving these properties.

### Acknowledgement

The Authors would like to thank the Iran National Science Foundation (INSF) for support of this project under, Proposal number 94027859.

## References

- [1] P. Joensen, R. F. Frindt, S. R. Morrison, *Mater. Res. Bull.*, 21, 457 (1986).
- [2] Uni O. Aqueous Suspension and Characterization of Chemically Modified Graphene Sheets 2008:6592–4.
- [3] M. Amini M, A. ARS, M. Faghihi, S. Fattahpour, Preparation of nanostructured and Nanosheets of MoS<sub>2</sub> oxide using ox- idation method. Ultrason - Sonochemistry 2017.
- [4] R. Rosentsveig, A. Gorodnev, N. Feuerstein, H. Friedman, A. Zak, N. Fleischer, et al. *Tribol. Lett.*, 36, 175 (2009).
- [5] Z. K. Su, Y. H. Cui, X. H. Tang, Q. Zhou, Z. H. Liu, Chinese. *J. Chem.*, 26, 575 (2008).
- [6] L. T. Eunju, E. L. Kee, S. J. Jong, B. Y. Kyung, *J. Am. Chem. Soc.*, 130, 6534 (2008).
- [7] S. M. Paek, H. Jung, M. Park, J. K. Lee, J. H. Choy, *Chem. Mater.*, 17, 3492 (2005).
- [8] M. Mirzaei, *Zeitschrift. Fur. Naturforsch. - Sect A. J. Phys. Sci.*, 65, 844 (2010).
- [9] J. Tannous, F. Dassenoy, I. Lahouij, T. Le Mogne, B. Vacher, A. Bruhács, et al. *Tribol. Lett.*, 41, 55 (2011).
- [10] H. I. Karunadasa, E. Montalvo, Y. Sun, M. Majda, J. R. Long, C. J. Chang, *Sci.*, 335, 698 (2012).
- [11] M. Wang, G. Li, H. Xu, Y. Qian, J. Yang, *A. C. S. Appl. Mater. Interfaces.*, 5, 1003 (2013).
- [12] F. Maugé, J. Lamotte, N. S. Nesterenko, O. Manoilova, A. A. Tsyanenko, *Catal. Today.*, 70, 271 (2001).
- [13] Q. Farhad, *J. Ind. Eng. Chem.*, 5, 1 (2015).
- [14] S. C. Shi, J. Y. Wu, T. F. Huang, *Opt. Quantum. Electron.*, 48, 474 (2016).
- [15] Rong J, Sheng MIA, Li H, Ruckenstein ELI. Po lye t hy I ene- Pa I y g ors kite Na nocom p Os it e Prepared via in situ Coordinated Polymerization n.d.;2:658–65.
- [16] M. Amini, et al. Materials Today: Proceedings 5.7 (2018): 15613-15619.
- [17] P. Zapata, R. Quijada, C. Covarrubias, E. Moncada, J. Retuert, D. Lee, et al. *Appl. Clay. Sci.*, 113, 457 (2008).
- [18] A. Dashti, A. Ramazani SA, Y. Hiraoka, S. Y. Kim, T. Taniike, *Macromol. Symp.*, 285, 52 (2009).
- [19] M. Shafiee, A. Ramazani AS, H. Bahrami, A. Kheradmand, *R. S. M.*, 11, 55 (2014).
- [20] M. Amini, et al. Polymers for Advanced Technologies (2018).
- [21] A. Kheradmand, A. Ramazani S.A., F. Khorasheh, M. Baghalha, H. Bahrami, *Polym. Adv. Technol.*, 26, 315 (2015).
- [22] H. Bahrami, A. Ramazani AS, A. Kheradmand, M. Shafiee, H. Baniasadi, *Adv. Polym.*

*Technol.* 34, 1 (2015).

- [23] J. Chen, F. Maug, E. I. J. Fallah, L. Oliviero, *J. Catal.*, 320, 170 (2014).
- [24] S. K. Ghosh, C. Srivastava, S. Nath, J. P. Celis, *Int. J. Electrochem.*, 20, 1 (2013).
- [25] M. Del Valle, J. Cruz-Reyes, M. Avalos-Borja, S. Fuentes, *Catal. Letters.*, 54, 59 (1998).
- [26] B. C. Helmlly, W. E. Lynch, D. A. Nivens, *Spectrosc. Lett.*, 40, 483 (2007).
- [27] S. Kazuo, T. S. Yoshiharu Doi, *Makromol. Chem.*, 189, 1531 (1988).
- [28] G. H. Zohuri, R. Jamjah, S. Ahmadjo, *J. Appl. Polym. Sci.*, 100, 2220 (2006).
- [29] P. PokasermSong, P. Praserthdam, *Eng. J.*, 13, 57 (2009).
- [30] H. Baniasadi, A. Ramazani S.A., S. Javan Nikkhah, *Mater. Des.*, 31, 76 (2010).
- [31] J. R. H. Li, Z. Jing, X. Hong, M. Sheng, *J. Appl. Polym. Sci.*, 82, 1829 (2001).